REAL-TIME R-SPIKE DETECTION IN THE CARDIAC WAVEFORM THROUGH INDEPENDENT COMPONENT ANALYSIS

Harold Martin, Walter Izquierdo, Mercedes Cabrerizo, and Malek Adjouadi
Center for Advanced Technology and Education, Department of Electrical and Computer Engineering
Florida International University, Miami, FL, USA
hmart027@fiu.edu; walter.izquierdo@gmail.com; mcabreriz@fiu.edu; adjouadi@fiu.edu

***Abstract*—Electrocardiograms (EKGs) are the most common diagnosis tools used for the detection and diagnosis of cardiovascular diseases and abnormalities. In this paper, we proposed a method that uses independent component analysis (ICA) for the real-time detection of the most distinct component of the cardiac electrical signal, the R-peak. This approach will open the door to real-time analysis and decomposition of the complete cardiac signal and the online diagnosis of cardiac abnormalities. The potential benefits of such real-time implementation are far reaching, from the online diagnosis of diseases and abnormalities to its use in tracking heart functioning during the testing and development of cutting edge research and treatments, such as transcranial magnetic stimulation (TMS).**

Keywords—ECG; EKG; ICA; R-peak; Real-time processing; cardiovascular disease; real-time detection; TMS;

I. INTRODUCTION

Electrocardiograms (EKGs) are the most common diagnosis tools used for the diagnosis of heart diseases. They are a representation of the heart's electrical signal and therefore, convey relevant information about the condition of such vital organ. Physicians are often challenged when searching for heart disease biomarkers among the complex EKG signals. Due to the extension of the common data and the sparsity of some of these patterns, the task of identifying proper biomarkers becomes hard, exhaustive, and time consuming. EKGs, as most biomedical signals, are affected by various noise levels that hinder the accuracy and feasibility of automatic detection of such patterns and often result in lots of misdetections and incorrect diagnosis. Therefore, the accurate detection and localization of cardiac signal components, as well as the known biomarkers, is of special interest for EKG analysis.

Several attempts have been made at automatic R-peak detection and multiple strategies have been developed for effective noise removal [1-5]. R-peak detection is especially useful as a starting point for the decomposition of the cardiac signal into its subcomponents and it is also useful to determine and diagnose conditions associated with abnormal cardiac rhythms [6,7]. Therefore, real-time detection of R-peaks would be extremely beneficial to the analysis of the heart, as it would enable the online diagnosis and detection of abnormalities associated with the cardiac rhythm.

Independent Component Analysis (ICA) decomposition has played a historically leading role in biosignal denoising, especially where the observed signals are assumed to be mixtures of originally independent sources [8-12]. This statistical technique is widely applied in other disciplines such as electroencephalogram (EEG) signal denoising. Where, in our opinion, by isolating foreign sources of noise it achieves the most promising artifact removal results [8,10].

ICA is often used during the pre-processing phase to remove noise and external perturbations to the signal that degrade the detection process [10-12]. It is a very powerful tool that allows us to separate the independent sources present in mixed signals. However, due to the nature of ICA the separation matrix is often randomly initialized, resulting in independent sources that are differently ordered every time the algorithm is performed.

This signal processing algorithms are often performed offline, over an entire record, and in the background, where the physicians do not have access to the decision process of what is noise and what is not. This is a common drawback of filtering techniques that might lead to the loss of important information.

In this paper, we propose a slightly different use of ICA for electrocardiogram analysis and R-peak detection. ICA benefits from signals recorded from different points of views, yielding the same number of independent sources as there are mixed signal. Therefore, a 12-lead EKG will yield 12 independent components, one of which is bound to be the R-peaks, as they are the most distinctive feature of the EKG. Our approach separates the components of the cardiac electrical signal and applies the detection process on them. This approach preserves all the lead's recordings of the signal for observation and validation while still performing heart disease biomarker detection over the independent components. The potential benefits of such real-time implementation are far reaching, from the online diagnosis of diseases and abnormalities to its use in tracking heart functioning during the testing and development of cutting edge research and treatments, such as transcranial magnetic stimulation (TMS)[15].

The method proposed in this study focuses on the detection of the R-peak in the PQRST complex.

II. METHODS

A. The Data

The data used for the development of this method was provided by The PTB Diagnostic ECG Database [13, 14]. It consists of a collection of 549 records from 290 subjects. Ages ranged from 17 to 87 with a mean of 57.2. There are 209 men and 81 women. Each record contains 15 simultaneously measured signals: the conventional 12 leads (i, ii, iii, avr, avl, avf, v1, v2, v3, v4, v5, v6) and 3 Frank lead ECGs (vx, vy, vz). The signals were sampled with a 16-bit ADC at 1000 samples per second, over a range of ± 16.384 mV. There is also a clinical diagnosis associated with most of the records. The diagnosis available are: Myocardial infarction (148), Cardiomyopathy/Heart failure (18), Bundle branch block (15), Dysrhythmia (14), Myocardial hypertrophy (7), Valvular heart disease (6), Myocarditis (4), Miscellaneous (4), Healthy controls (52).

B. Data Filtering

The best noise to have is none. However, sources of noise are always present and we must deal with their interference. Some noise sources (i.e. power line interference) can be relatively easy to remove, others present more of a challenge and can lead to unwanted consequences (i.e. muscle movements capture by equipment, eye blinks in EEGs), and some are unavoidable (i.e. signals emanating from an unknown source, or simply unwanted interference that we could be unaware of).

The simples noise sources to deal with are external, i.e. the environment, AC power lines, lighting, and interference from various electronic equipment. When recording EKGs, we are interested in a very specific set of electrical signals generated by the functioning of the heart, all other signals that are not related to it are simply noise and hinder our ability to perform proper processing.

Several methods have been proposed to deal with noise removal over past decades. The process of filtering can be performed either in the time or frequency domain and some of the most widely used techniques to do so are noise subtraction using linear regression, adaptive filtering, and data decomposition.

In this study, we use simple filters, a 60Hz stop-band Infinite Impulse Response (IIR) to remove power line interference and a 500 milliseconds rolling average filter to reduce low frequency noise.

C. Independent Component Analyis

The key assumption of Blind Source Separation (BSS or independent component analysis) is that the observed signals are a mixture of originally independent sources. There are different approaches that differ in the algorithms and the information used to estimate the mixing matrix and the source signals.

Second order statistics methods are based on the assumption that the original signal sources are uncorrelated and aim to decompose the observed signals into several uncorrelated components. Principal Component Analysis (PCA), perhaps the most widely known method, decomposes a given time series into a number of orthogonal (uncorrelated) components of decreasing significance, such that most of the variance of the original signal is contained by a small subset of the principal components (the components with highest corresponding eigenvalues). PCA is most often used as a dimensionality reduction method.

When the original signal sources are assumed to be independent, methods based on higher order statistics can be used to decompose the observed signals. Various methods that make use of various measures of statistical independence for independent component analysis (ICA) have been developed [8, 16].

An independent component analysis method searches for a linear transformation that minimizes the statistical dependence between the components of a given signal. The expansion of mutual information is utilized as a function of cumulants of increasing orders to define a suitable search criterion [7].

Suppose we have a random variable S, with probability density function $P_s(s)$, and the cumulative distribution function $F(s) = P(S \leq s)$ defined as:

$$F(s) = \int_{-\infty}^{s} P_s(t)\, dt \quad \text{or} \quad P_s(s) = F'(s) \qquad (1)$$

Therefore, we can model the distribution of the variable S either by specifying its probability density functions or its cumulative distribution function.

Assuming the data comes from n original sources, meaning $S \epsilon \mathbb{R}^n$ (n different parts of the heart), we define $s_k^{(i)}$ as the signal from the independent component k at time i.

What we observe in the EKG recording is an actual combination of the independent sources (assuming linearity and ignoring propagation speed differences as well as conductance disparities for simplicity):

$$X^{(i)} = A * S^{(i)} \quad (2)$$

where $X^{(i)} \epsilon \mathbb{R}^n$ corresponding to the n electrodes. Here the matrix A is known as the mixing matrix and what we observe at the j^{th} electrode at time i is:

$$x_j^{(i)} = \sum_k A_{jk} s_k^{(i)} \quad (3)$$

The goal of the ICA method is to find the optimal un-mixing matrix $W = A^{-1}$ so that we can recover the original sources from the observable variables:

$$S^{(i)} = W * X^{(i)} \quad (4)$$

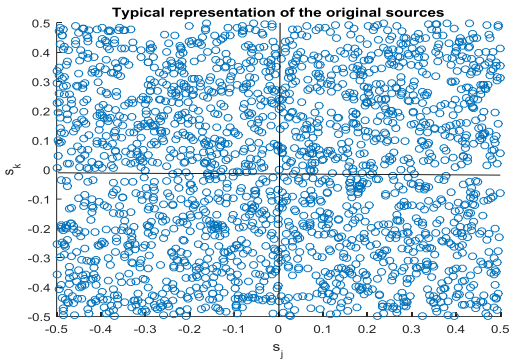

Figure 1. Independent Components

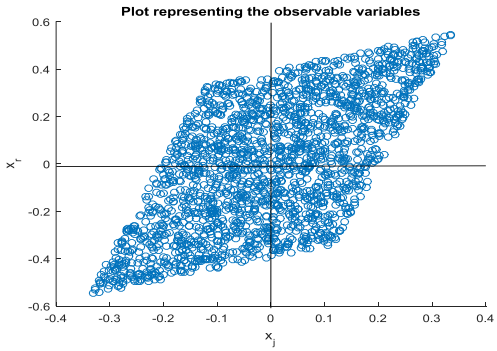

Figure 2. Mixture of Independent Components

To further illustrate this, let's suppose each of my original sources (independent signals) are random white noise. This way, we can think of a 2D plot of any of the sources as the plot represented in Figure 1. On the other hand, a typical sample of what is recorded by the electrodes is represented in Figure 2.

The purpose of ICA is to find the transformation ($matrix\ W$) that would obtain Figure 1 from Figure 2. Since the original sources are independent, the probability density function of s is going to be given by the product of the marginal probabilities of each s_i:

$$P(s) = \prod_{i=1}^{n} P_s(s_i) \quad (5)$$

Then the density for X will be:

$$P(x) = [\prod_{i=1}^{n} P_s(w_i{}^T x)] * |W| \quad (6)$$

Where $w_i{}^T$ is the i^{th} row of the W matrix.

To complete the formulation of the ICA model, it is necessary to choose a probability density function for the sources s_i. What is usually selected is the cumulative distribution function as any signal that goes from zero to one. State-of-the-art ICA algorithms use a variety of functions. Some of them maximize one of the following: non-gaussianity, independence, or complexity.

The complete ICA model then follows as:

Given my training set $\{x^1, x^2, \dots, x^n\}$, we can derive the log likelihood of the parameters as:

$$l(W) = \sum_i \log(\prod_j P_s(w_i{}^T x)) * |W| \quad (7)$$

The stochastic gradient descent algorithm is used to arrive at the optimal mixing matrix W:

$$W_{k+1} = W_k + \propto \nabla_W l(W) \quad (8)$$

The proposed approach uses FastICA [17], a reputed ICA algorithm that relies on the maximization of non-gaussianity of the independent sources. Traditionally, the mixing matrix is randomly initialized but through experimentation we have observed that using the identity matrix as a starting point tends to result in the first independent component being the most distinctive feature of the electrocardiogram, the R wave.

The configuration of the electrodes is not subject to change during the collection of the data, and as such, the separation matrix of the signal should not change either. Therefore, we perform the ICA algorithm in the first 10 seconds of data and use the resulting separation matrix for the remainder of the collection. This allows us to perform real-time detection of the R peaks.

D. Modeling background interference and selection of R-peak candidates

The data used for this study comes from the recording of 12 distinct electrodes signals from different anatomical locations (which are transformed in to 12 signals). However, there can be many more co-occurring processes in the heart ($n \gg 12$). Since ICA inputs are these 12 signals, we can only recover 12 independent components out of the algorithm. Our assumption is that the R spikes are strong enough in the mixed signals in terms of frequency and amplitude that will be captured completely by a single component of the ICA transformation. We will call it the R-component. In other words, the R spikes are going to be represented and clearly observed in one of the independent components the ICA algorithm outputs. In the ideal case, meaning that there are only 12 undergoing processes in the heart, the R-component

will only capture the R spikes and only minimum noise should be observe. The real case scenario is that there still exist $n - 12$ independent relevant processes that have no option but to be distributed among the 12 independent components being extracted. This leads to non-minimal noise in each of the output signals, including the R-component. Proving that this noise is Gaussian might be tedious in terms of the applicability of the Central Limit theorem and the assumption on how this electrode signals are measured. Moreover, we do not plan to do statistical inferences based on normality assumptions. However, a near normal behavior could still be beneficial to somehow model and deal with this noise.

One empirical way to corroborate the normality assumption is to look at the histogram of the signal. We start by picking a random patient and obtaining the corresponding R-component signal. We then remove the extreme values that might correspond to the R-spikes or some other artifacts to leave only the supposed Gaussian noise behind. Figure 3 shows the histogram of this signal.

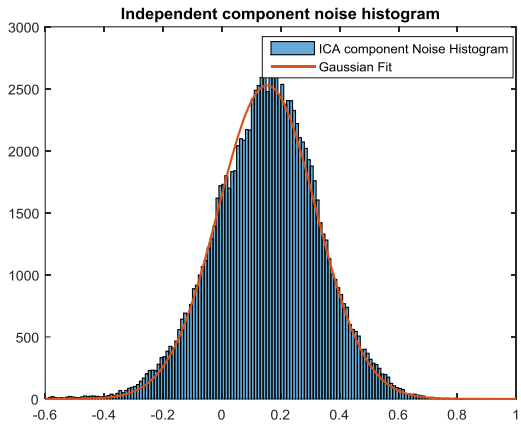

Figure 3. Histogram of the First Independent Component

It can be seen from the figure, that the normality assumption is not a bad approximation. The Q-Q plot for this signal is also provided in Figure 4.

It can be observed that there is a slightly deviation from normality at the lower quartiles resulting in a heavier left tale. This is likely due to the presence of noisy artifacts or the presence of any other independent source in this component. Either way, the normality assumption is still valid for our purposes.

This behavior is representative of all the patients in our study. We did not proceed any further with normality testing, as it would have not been very useful.

The normality assumption allows us to model this independent component as a Gaussian-distributed background signal with the R-peaks superimposed. As a consequence, whatever fits inside the Gaussian distribution is considered background noise, and those events not explained by the model (3 standard deviations or more away from the mean) are considered R-peak candidates.

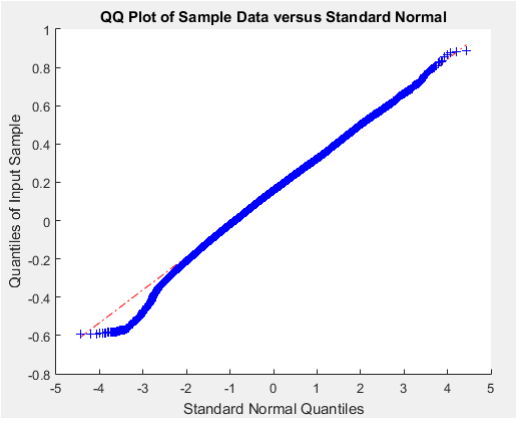

Figure 4. Q-Q plot of First Independent Component vs Standard Normal distribution

Taking advantage of the Normal distribution properties shown in the graph below, we can setup thresholds that would identify the occurrence of R-spikes:

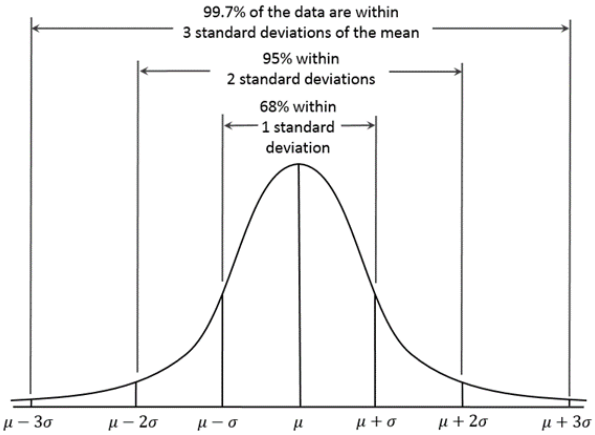

Figure 5. For the normal distribution, the values less than one standard deviation away from the mean account for 68.27% of the set; while two standard deviations from the mean account for 95.45%; and three standard deviations account for 99.73%. https://en.wikipedia.org/wiki/Normal_distribution

Therefore, we proceed by computing the mean μ_j and the standard deviation σ_j of a 500 milliseconds rolling window in the selected component.

Following the model of the Gaussian distribution visualized in the figure, we can conclude that 99.7% of the noise will be within the $[\mu_j - 3 * \sigma_j,\ \mu_j + 3 * \sigma_j]$ range and any point that lays outside it is a possible R-peak candidate. Therefore, the algorithm tests for the following condition:

$$\begin{cases} if \quad \mu_j - 3 * \sigma_j \leq s_j^{(i)} \leq \mu_j + 3 * \sigma_j \\ the\ i^{th}\ sample\ of\ the\ j^{th} is\ a\ spike\ candidate \\ otherwise\ it\ is\ not\ a\ spike\ candidate \end{cases} \quad (9)$$

Where the application of this condition leads to a set of possible R-peak candidates.

The last detection step is to check whether the width of the proposed peaks is within 10 and 60 milliseconds. Figure 6 shows the first independent component (in black) alongside the rolling threshold (blue, as defined by the condition in equation 9).

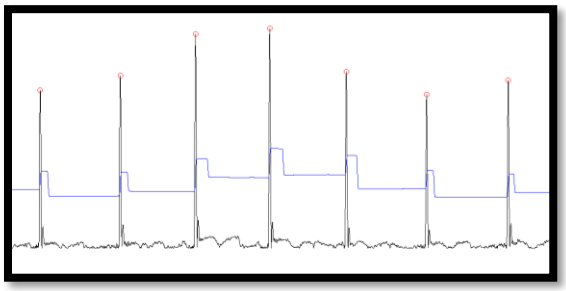

Figure 6. R-peak detection in First Independent Component (black) and Detection Threshold (blue)

III. Results

Initial experimental results and analysis can be reported for a subset of 80 randomly selected recording from the 549 available. Said sample is composed of 40 healthy individuals and 40 unhealthy ones with one or more diagnosis (myocardial infarction, cardiomyopathy/heart failure, bundle branch block, dysrhythmia, myocardial hypertrophy, valvular heart disease, myocarditis, miscellaneous). These records collectively contain over ten (10) thousand R waves. Table 1 contains the summary statistics for the proposed method over the processed records.

Subjects	True Positives	False Positives	False Negatives	Detection Rate (Sensitivity)
Controls	5,411	6	112	97.97%
Others	5,188	3	90	98.29%
Total	10,599	9	202	98.13%

Table 1. Summary Statistics for Proposed Method

We are unable to report accuracy readings from one of the files as it contains numerous artifact that make the proper labeling of the R-peaks (by humans) impossible. Figure 7 depicts a portion of such recording along with the attempts of the proposed algorithm to detect the R-peaks (red vertical bars). Figure 8 shows the computed threshold (blue line) and the independent component being looked at. Finally, Figure 9 show how the artifacts affect all the independent components extracted from the ECG.

For all other 79 files, the proposed method performed accordingly, properly identifying over 98 percent of the R-peaks. Most of the files containing false negatives misdetected only the first, or first two, beats while the rolling threshold was being initialized. Only 8 EKG records had more than three (3) false negatives.

Figure 7. EKG Record 557 for patient 293. It contains multiple artifacts that make proper R-peak labeling impossible.

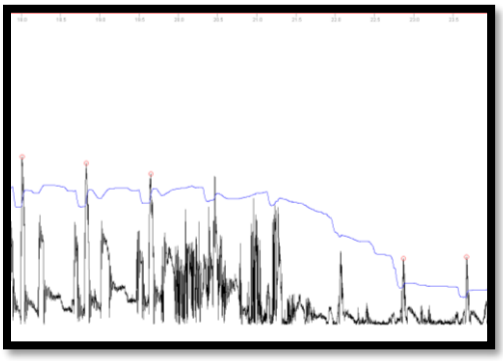

Figure 8. Second Independent Component (black) along with the computed rolling threshold (blue) for Figure 7.

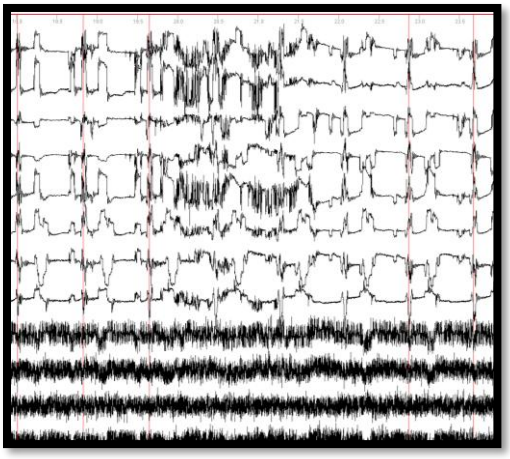

Figure 9. Independent Components of EKG Record 557 for patient 293. It shows how the artifacts from the EKG affect all components effectively not allowing the proposed method to extract or identify the R-peaks when they are present.

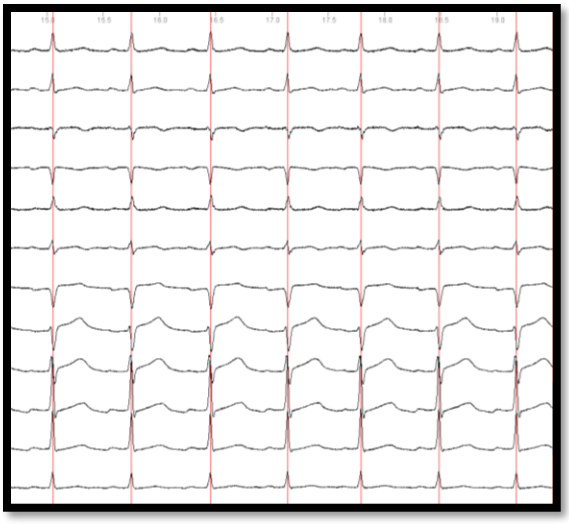

Figure 10. EKG Record 242 for patient 75. It is an EKG from a patient with a Myocardial Infarction.

Figure 11. Independent Components of EKG Record 242 for patient 75.

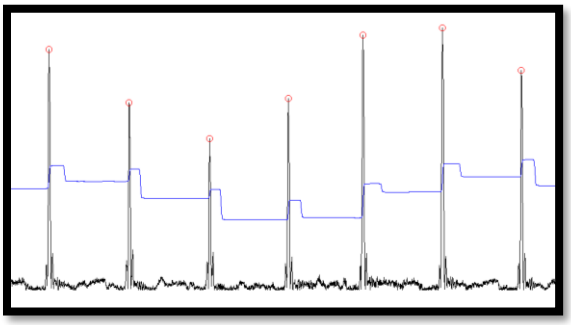

Figure 12. Second Independent Component (black) along with the computed rolling threshold (blue) for Figure 10.

Figures 10 through 12 show how the algorithm detects the R-peaks. Figure 10 contains the 12-lead input EKG with the R-peaks labeled (red vertical bars), figure 11 is the results of applying independent component analysis to the input signal in 10, and figure 12 demonstrates how the proposed rolling threshold works when identifying potential R-peak candidates in the identified independent component.

Another key example is how the algorithm ignores signal artifacts, as they would tend to a component different than the one containing the R-peaks. Figure 13 is such a case, where unrecognized artifact, that could hinder the accuracy of R-peak detection algorithms, are present and not detected as R-peaks. From figure 15, it is apparent that the artifacts affect the first three independent components but are rather attenuated in the fourth, where the R-peaks are. Figure 14, as in previous instances, shows the independent component containing the R-peaks (black) along with the moving threshold being computed (blue).

Figure 13. EKG Record 543 for patient 284. An EKG containing multiple artifacts that could hinder the performance of R-peak detection algorithms.

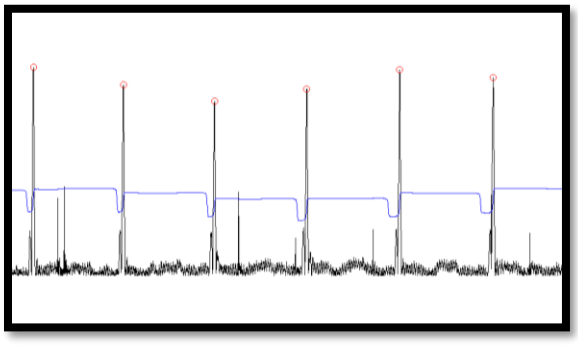

Figure 14. Forth Independent Component (black) along with the computed rolling threshold (blue) for Figure 13.

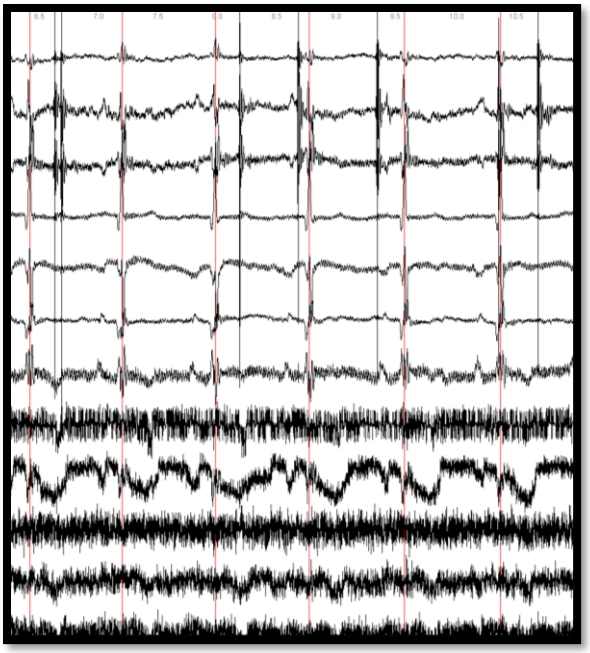

Figure 15. Independent Components of EKG Record 543 for patient 284.

When the EKG waveform contains significant perturbations, the first component could capture a signal other than the R-peaks. This is the case for some records of patients with myocardial infarction and some controls that contained significant artifacts were the first component would alternate between the Q, R, and S spikes, and the component containing the R-peak could be as far back as the third one. Table 2 is a summary of the location of the R-peaks within the independent components.

	IC1	IC2	IC3	IC4
#of EKGs	63	15	1	1

Table 2. Number of EKGs containing the R-peak in the given Independent Component

Although the R-peaks fall to the first independent component in most instances, a procedure to automatically identify its location, or force them to appear in the first IC all the time, remains as future work.

IV. Conclusions

We have proposed an algorithm for the real-time detection of the most distinct component of the cardiac electrical signal, the R-peak. It implements independent component analysis (ICA) to isolate the source of this signal and a rolling threshold to select potential candidates. This approach could lead to real-time analysis and decomposition of the complete cardiac signal and the online diagnosis of cardiac abnormalities. The potential benefits of such real-time implementation are far reaching, from the online diagnosis of diseases and abnormalities to its use in tracking heart functioning during the testing and development of cutting edge research and treatments, such as transcranial magnetic stimulation [15].

V. Acknowledgments

We acknowledge the critical support provided by the National Science Foundation under grants: CNS-1532061, CNS-1551221, CNS-1042341, IIP 1338922, and CNS-1429345. The generous support of the Ware Foundation is greatly appreciated. Harold Martin is supported through the NSF Graduate Fellowship Program (GRFP) DGE-1610348.

Any opinion, findings, and conclusions or recommendations expressed in this material are those of the authors(s) and do not necessarily reflect the views of the National Science Foundation.

VI. References

[1]. J.S. Park, SW Lee, U. Park "R Peak Detection Method Using Wavelet Transform and Modified Shannon Energy Envelope", JOURNAL OF HEALTHCARE ENGINEERING, 2017

[2]. YR. Ma, TQ. Li, YD. Ma, K. Zhan "Novel Real-Time FPGA-Based R-Wave Detection Using Lifting Wavelet" CIRCUITS SYSTEMS AND SIGNAL PROCESSING, Vol: 35 Issue: 1 pp. 281-299 Published: JAN 2016

[3]. S. Rekik, N. Ellouze "Enhanced and Optimal Algorithm for QRS Detection" IRBM Volume: 38 Issue: 1 pp. 56-61 Published: FEB 2017

[4]. V. Abromavicius, A. Serackis "Algorithm for Real-Time Detection of Heart Rate from Noisy ECG Signals Supported by Continuous Blood Pressure Analysis" 2015 OPEN CONFERENCE OF ELECTRICAL, ELECTRONIC AND INFORMATION SCIENCES (ESTREAM) Published: 2015

[5]. S. Sahoo, P. Biswal, T. Das, S. Sabut "De-noising of ECG Signal and QRS Detection using Hilbert Transform and Adaptive Thresholding" Book Series: Procedia Technology Vol: 25 pp. 68-75 Published: 2016

[6]. L. D. Sharma and R. K. Sunkaria, "A robust QRS detection using novel pre-processing techniques and kurtosis based enhanced efficiency," Measurement, vol. 87, pp. 194–204, 2016.

[7]. Y.-C. Yeh and W.-J. Wang, "QRS complexes detection for ECG signal: the difference operation method," Computer Methods and Programs in Biomedicine, vol. 91, pp. 245–254, 2008.

[8]. Nian Zhang and Jing Nie, "Independent component analysis based blind source separation algorithm and its application in the gravity and magnetic signal processing," 2015 12th International Conference on Fuzzy Systems and Knowledge Discovery (FSKD), Zhangjiajie, 2015, pp. 269-273.

[9]. L. de Lathauwer, B. de Moor and J. Vandewalle, "Fetal electrocardiogram extraction by blind source subspace separation," in IEEE Transactions on Biomedical Engineering, vol. 47, no. 5, pp. 567-572, May 2000.

[10]. M. B. Hamaneh, N. Chitravas, K. Kaiboriboon, S. D. Lhatoo and K. A. Loparo, "Automated Removal of EKG Artifact from EEG Data Using Independent Component Analysis and Continuous Wavelet Transformation," in IEEE Transactions on Biomedical Engineering, vol. 61, no. 6, pp. 1634-1641, June 2014.

[11]. MQ. Chen, X. Zhang, X. Chen, MX. Zhu "FastICA peel-off for ECG interference removal from surface EMG" BIOMEDICAL ENGINEERING ONLINE Vol. 15 Article Number: 65 Published: JUN 13 2016

[12]. U. Nelakuditi "Removal of Ocular Artifacts in EEG" PROCEEDINGS OF THE 10TH INTERNATIONAL CONFERENCE ON INTELLIGENT SYSTEMS AND CONTROL (ISCO'16) (2016)

[13]. R. Bousseljot, D. Kreiseler, A. Schnabel, "Nutzung der EKG-Signaldatenbank" CARDIODAT der PTB über das Internet. Biomedizinische Technik, Band 40, Ergänzungsband 1 (1995) S 317

[14]. Goldberger AL, Amaral LAN, Glass L, Hausdorff JM, Ivanov PCh, Mark RG, Mietus JE, Moody GB, Peng C-K, Stanley HE. PhysioBank, PhysioToolkit, and PhysioNet: Components of a New Research Resource for Complex Physiologic Signals. Circulation 101(23): e215-e220 [Circulation Electronic Pages; http://circ.ahajournals.org/content/101/23/e215.full]; 2000 (June 13).

[15]. M. Cabrerizo, A. Cabrera, J.O. Perez, J. de la Rua, N. Rojas, Q. Zhou, A. Pinzon-Ardilla, S.M Gonzalez-Arias, and A. Malek "Induced Effects of Transcranial Magnetic Stimulation on the Autonomic Nervous System and the Cardiac Rhythm" The Scientific World Journal. Vol. 2014, pp. 349718, Published: 2014 (Epub 2014 Jul 17)

[16]. G. Repovs "Dealing with Noise in EEG Recording and Data Analysis". Informatica Medica Slovenica 15(1), 2010

[17]. T. Wei, "A convergence and asymptotic analysis of the generalized symmetric FastICA algorithm". IEEE Transactions on Signal Processing. Vol. 63, Issue 24: 6445-6458, 2015